The Composition of Emissions from Sanding Corian® with Different Sandpapers

Seungkoo Kang[1], Huayan Liang[1], Yong Qian[2], Chaolong Qi[1]

[1] Centers for Disease Control and Prevention, National Institute for Occupational Safety and Health, Division of Field Studies and Engineering, Cincinnati, OH 45226, USA
[2] Centers for Disease Control and Prevention, National Institute for Occupational Safety and Health, Health Effects Laboratory Division, Morgantown, WV 26505, USA

ABSTRACT

Laboratory tests were conducted to characterize the composition of emissions from sanding Corian®, a solid-surface composite material mainly composed of alumina trihydrate (ATH) and acrylic polymer. Three sandpaper materials (ceramic, silicon carbide, and aluminum oxide) were tested to distinguish the contribution of aluminum-containing dust in the emission from Corian® and sandpaper itself. The result can help identify the main cause of the pulmonary fibrosis from exposure to aluminum-containing dust while sanding Corian®. Airborne dust samples were measured using direct-reading instruments and collected using a Micro-Orifice Uniform Deposit Impactor (MOUDI) for estimating the normalized dust generation rate. The size-classified dust samples from MOUDI were analyzed for elemental aluminum content. Additionally, air samples were analyzed for characterizing methyl methacrylate (MMA). The results from the direct-reading instruments reveal that the size distribution of particulate from sanding Corian® differs from that of sawing Corian®, showing that the size distribution of dust is affected by the fabrication process. The normalized respirable dust generation rate indicates that more respirable dust was generated during sanding Corian® board. However, the use of aluminum oxide sandpaper does not result in a higher aluminum content in the respirable dust from sanding Corian®, suggesting that the aluminum content of the respirable dust is primarily originated from Corian® itself. The generation rates of MMA from sanding did not vary much among all types of sandpapers, and they were much lower than that of sawing, likely due to the higher temperature in the sawing process.

Keywords: Solid-surface composite, Respirable dust, Alumina trihydrate, Sanding

1 INTRODUCTION

Corian® is a widely used solid-surface composite material that is often used for countertops. Its product overview (DuPont, 2018) specifies that it is mainly composed of about 1/3 acrylic resin (polymethyl methacrylate) and about 2/3 alumina trihydrate (ATH). Countertop fabrication processes, including sanding and sawing, may pose an occupational risk for workers as they are exposed to emissions containing respirable dust and volatile organic compounds (VOCs). Exposure to these emissions is associated with respiratory and cardiovascular morbidity (Brook *et al.*, 2010). In addition, inhalation of metal dust including aluminum can cause pulmonary fibrosis (Kelleher *et al.*, 2000; Taskar and Coultas, 2006).

A pulmonary fibrosis case associated with exposure to ATH dust was reported for a worker who had worked with Corian® (Raghu *et al.*, 2014). However, McKeever *et al.* (2014) raised a question whether the main cause of the pulmonary fibrosis was ATH from Corian® or the aluminum oxide from sandpapers. In order to find the main cause of the pulmonary fibrosis, we conducted systematic studies as follows. Qi *et al.* (2016) investigated the emissions from sawing Corian® by measuring the size distribution of the airborne dust and aluminum content in total

airborne and respirable dust samples. The results indicated that ATH was dominant in both respirable and total airborne dusts, and a large amount of ultrafine particles was generated. Kang *et al.* (2019) further studied the emissions from sawing Corian® by collecting size-classified airborne dust samples and analyzing ATH distribution in the dust of different sizes. For most parts of the respirable size range, the ATH content was above 85%, thus confirming that aluminum in the respirable dust, including ultrafine particles, mainly comes from Corian®.

In order to further verify whether sandpaper could contribute significantly to the respirable dust that contains aluminum when sanding Corian®, we characterized the dust from sanding Corian® using three different sandpaper materials: ceramic, silicon carbide, and aluminum oxide. We collected size-selective airborne dust samples for the measurement of their size and the analyses of their aluminum contents. We also conducted analyses of VOCs in the emissions.

2 MATERIALS AND METHODS

2.1 Laboratory Testing System

We conducted the laboratory characterization of airborne particles by sanding Corian® in an automated laboratory testing system that is described in previous publications (Qi *et al.*, 2016; Kang *et al.*, 2019). Fig. 1 shows a schematic of the system configuration and its operation condition. An air handling unit (PSKB-1440, ProVent LLC, Harbor Springs, MI, USA) was used to generate airflow through a panel of pre- and HEPA filters for the removal of airborne particles before entering an automatic tool testing chamber. For each test, the flowrate in the chamber was set to 0.64 m^3 sec^{-1} by adjusting the blast gate valve, and a delta tube (306AM-11-AO, Midwest Instrument, Sterling, MI, USA) on the duct monitored the flowrate through the testing chamber. During the test, Corian® boards were automatically sanded by a Porter cable belt sander (Model 352VS, Porter Cable, Jackson, TN, USA) in the chamber using different types of sandpapers. For each sanding path, a dust cloud was generated and then carried downstream by the airflow through the testing chamber. The dust cloud was sampled through an isokinetic sampling probes on the duct of the testing system. The system was designed and operated in accordance to the European Standard EN 1093-3 (CEN, 2006) to sample a representative part of the airborne contaminants in the airflow. The volume flowrate used in this study was sufficient to keep the inhalable particles remain airborne according to this standard.

2.2 Belt Sander and Sandpapers

A Porter Cable belt sander was installed in the testing chamber for all the tests. Sandpapers of
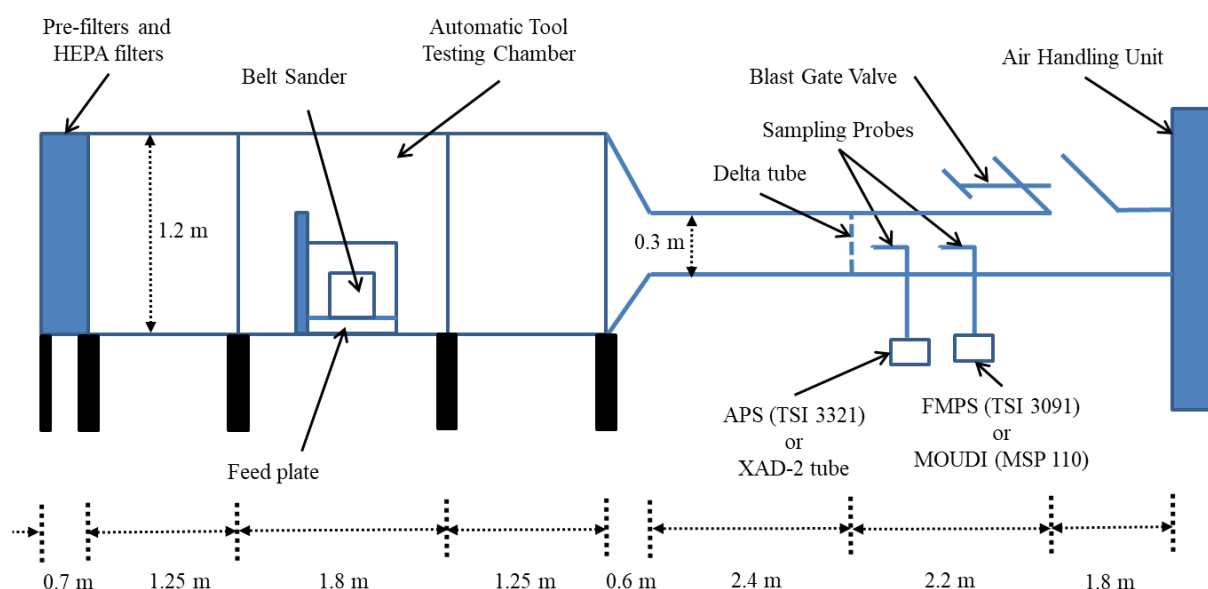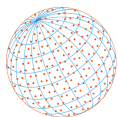

Fig. 1. Laboratory testing system.

three different materials including ceramic, silicon carbide, and aluminum oxide were tested. All tested sandpapers are 7.62 cm (3 inches) by 53.34 cm (21 inches) and had a grit size of 120 (Red Label Abrasives, MI, USA).

For each sanding test, the automatic tool-testing chamber was programmed to perform a pre-determined number of sanding pass cycles. Each sanding pass cycle included the following steps: 1) the feed plate fed the board forward; 2) power was supplied to the sander; 3) the 2D actuator moved the sander and made a sanding pass across the board; 4) the sander was turned off; and 5) the 2D actuator moved the sander back to its original position. A waiting time about 5 seconds was programmed between steps 2) and 3) to ensure the sander reached the designed speed before making a sanding pass. For each test, sanding was repeated more than 150 sanding pass cycles to obtain a statistically reliable amount of data, and new sandpaper was installed before conducting the next test. The operating condition of the belt sander remained the same for all experiments.

2.3 Sampling Method

Three sets of size-classified airborne dust samples were collected using a Micro-Orifice Uniform Deposit Impactor (MOUDI 110, TSI Inc, Shoreview, MN, USA) from a sampling port with a flowrate of 30 L min^{-1}. An isokinetic sampling probe was specifically designed and used for the MOUDI to obtain representative airborne dust samples. The MOUDI was equipped with pre-weighed PVC filters (47-mm diameter, 5-µm pore-size) and separates particulate matter into 12 different stages with the following cutoff points for each stage: 18, 10, 5.6, 3.2, 1.8, 1.0, 0.56, 0.32, 0.18, 0.1, 0.056 µm, and a final filter. The mass of the collected dusts on each filter was determined by post-weighing the filters. After gravimetric analysis, elemental aluminum analysis of each sample was conducted according to NIOSH Method 7303 (NIOSH, 2003a).

In addition to sampling size-selected dust samples, a Fast Mobility Particle Sizer Spectrometer (FMPS, Model 3091, TSI Inc., Shoreview, MN, USA) and an Aerodynamic Particle Spectrometer (APS, Model 3321, TSI Inc., Shoreview, MN, USA) were used to obtain real-time size distributions of the airborne dust from sanding Corian®. FMPS measures mobility diameter in the size range of 6–523 nm, while APS measures aerodynamic diameter in the size range of 0.542–19.8 µm. The time resolution during the measurement was 1 sec, which allowed both instruments to capture the entire dust cloud profile for each individual sanding pass, and to avoid overlaps of measurements between two adjacent sanding passes. As shown in Fig. 1, the APS took samples from the duct through an isokinetic sampling probe designed for its operating flowrate, while the FMPS used the sampling port and a probe that is designed to take isokinetic sample at 9.0 L min^{-1}. The operating flowrate of the FMPS is 10.0 L min^{-1}, so its sampling was anisokinetic. However, the maximum sampling bias (for particles of 523 nm) from the anisokinetic sampling was estimated about only 0.1% by the equation from Belyaev and Levin (1974). Measurements were repeated 10 times for each test. In addition, a baseline test with the belt sander running while not sanding Corian® was conducted to investigate the particles released from the running sander alone. Both APS and FMPS measure number-based size distributions directly. The mass-based size distributions were then obtained by assuming all the particles are spherical with a known density. The chemical composition of the particles generated from the baseline test was not analyzed so unit density was assumed for them. The analysis of the filter samples suggested that ATH is likely the dominant component of the airborne dust from sanding Corian® board, thus the density of ATH (2.42 g cm^{-3}) was used to derive the mass-based distributions for the dust from sanding Corian® board.

The previous study on sawing Corian® found that methyl methacrylate (MMA) was the most abundant VOC compound in the emissions with a very small generation rate. This is not a surprise as MMA's polymer form, i.e., polymethyl methacrylate is about 1/3 for the composition in Corian®. Therefore, we only sampled MMA from sanding in this study by collecting air samples in nine XAD-2 sorbent resin tubes (SKC Inc., Eighty four, PA, USA) with three samples for each sandpaper material. The MMA sampling was conducted in accordance with NIOSH Method 2537 (NIOSH, 2003b).

In this study, the generation rate is used to compare the data obtained from sampled dust and MMA. The normalized generation rate (G) of airborne contaminants (either dust or MMA) from
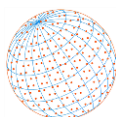
sanding Corian® board is defined as:

$$G = \frac{M_{sample} \cdot Q}{M_{loss} \cdot Q_{sampler}}$$

(1)

where, M_{sample} is the mass of the airborne contaminant from the sample; Q is the volume flowrate in the testing system; M_{loss} is the mass of the Corian® board that was removed by sanding (obtained by pre-weighing and post-weighing the board); and $Q_{sampler}$ is the sampling flowrate for the samplers used (MOUDI for dust and sorbent tube for MMA). G represents the mass of the corresponding airborne contaminant generated per unit of mass of the Corian® removed from sanding.

3 RESULTS AND DISCUSSION

3.1 Dust Analyses

Fig. 2 shows the average particle size distribution measured by FMPS while sanding Corian®. Each data point is the averaged result of ten replicates, and each replicate is the averaged result obtained during the sanding operation of one sanding path cycle. Each error bar represents the standard deviation of the ten replicates. For the comparison purpose, the average particle size distribution from sawing Corian® from previous study (Qi *et al.*, 2016) is included. We would like to note that the particle concentrations from sawing Corian® presented here are slightly higher than those presented in the previous paper, which was averaged for the entire operational cycle of a sawing test including the "dead time" between the adjacent two cycles when the particle concentration was close to zero.

As shown in Fig. 2(a), baseline tests from both sawing and sanding demonstrate a similar trend. Most particles are smaller than 50 nm, which may be produced mainly from the motors of the power tools under the no-load mode. The number-based size distribution from sanding is clearly different from that of sawing. The particle concentration from sawing is considerably higher than those from sanding for the particles smaller than about 50 nm while it is lower for the larger particles. This result along with the result of baseline tests suggests that the fabrication process (sawing and sanding) indeed affects the size distribution of the generated particles. A smaller difference is observed between the size distributions from sanding using different sandpaper materials, with the concentration from the sandpaper of aluminum oxide being slightly higher than the other two. Compared to the sanding baseline test, the results shown in Fig. 2(a) suggests that most particles smaller than 30 nm are generated from the sander's motor, and larger particles are from sanding Corian®. The mass-based size distribution from sawing Corian® plotted
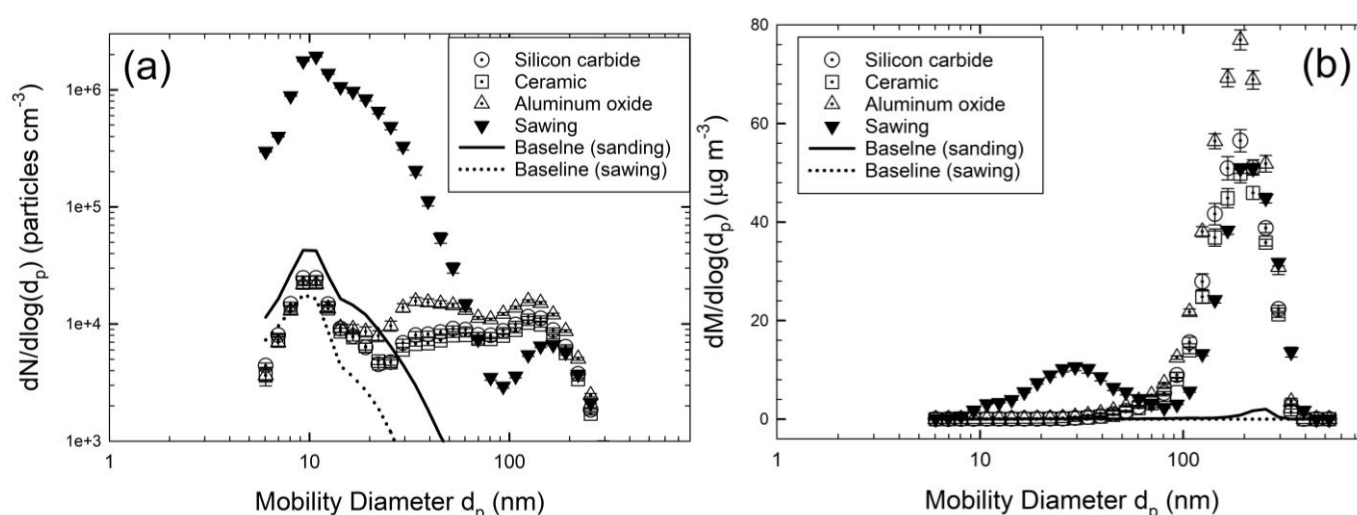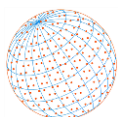

Fig. 2. (a) Number-based and (b) mass-based size distributions of the dust measured by FMPS from sawing and sanding (with sandpapers of ceramic, silicon carbide, and aluminum oxide) Corian®.

in Fig. 2(b) shows a bimodal distribution with modes of particle sizes at around 29 nm and 191 nm, while the distribution from sanding shows a unimodal distribution with a mode at around 191 nm. While their patterns in the mode of 191 nm are similar, the highest peak was found from aluminum oxide sandpaper and the lowest was found from sawing and sanding with ceramic sandpaper. Both baseline tests show an almost negligible amount of particle mass.

Fig. 3 shows the size distributions of particles generated from sanding and sawing measured by APS. All the data points are averaged from ten replicate measurements, and each error bar represent the standard deviation of the ten measurements. Both baseline tests show negligible amounts of particles in the particle size range of the APS. The number-based size distributions in Fig. 3(a) show a mode at around 1 μm from both sawing and sanding Corian®. Among all the results, the size distribution from sawing shows the lowest number concentration while that from sanding with aluminum oxide shows the highest number concentration. As shown in Fig. 3(b), the mass-based APS data shows bimodal distributions, while the mode of the smaller particle size is less apparent for the sawing result. The size distributions from sanding have the first mode at about 2.5 μm and the second at about 7.5 μm. In general, sanding with different sandpaper materials generates similar amounts of particle mass in the particle size range of the APS. Compared to sanding, sawing leads to higher mass concentration for particles larger than about 3 μm and lower mass concentration for smaller particles. Please note that the particle concentration levels shown in Figs. 2 and 3 can be different from the actual exposure data in practice, as they were obtained from the laboratory setting, although the shape of the particle size distributions are expected to be similar.

Fig. 4 illustrates the normalized generation rate G of the airborne dust and aluminum element in the dust generated from sanding and sawing Corian® board. The error bars in the plot are standard deviations of three MOUDI replicates. In general, the G from sawing is considerably lower than that from sanding. The G for airborne particles of different sizes from sanding is between 0.2 and 33.4 mg g^{-1}, while that from sawing is between 0.2 and 3.6 mg g^{-1}. The particle concentration levels illustrated in Fig. 3 have a much smaller difference between sanding and sawing. The larger difference on G shown in Fig. 4 suggests that sanding has a much larger portion of the materials removed from Corian® becoming airborne particles compared to sawing. This is consistent with the observation that sawing had a much larger amount of settled dust in the chamber. A similar pattern is observed among all the sanding results with their peaks at around 7.5 μm. The G for the ceramic sandpaper is the highest, and that for the aluminum oxide sandpaper is the lowest. The pattern for the G of aluminum element in the dust shown in Fig. 4(b) is similar to that of airborne dust in Fig. 4(a), suggesting that the aluminum content does not vary considerably among particles of different sizes. By considering the respirable fraction for each MOUDI stage, we derived the generation rate of respirable dust G_{rd} as:
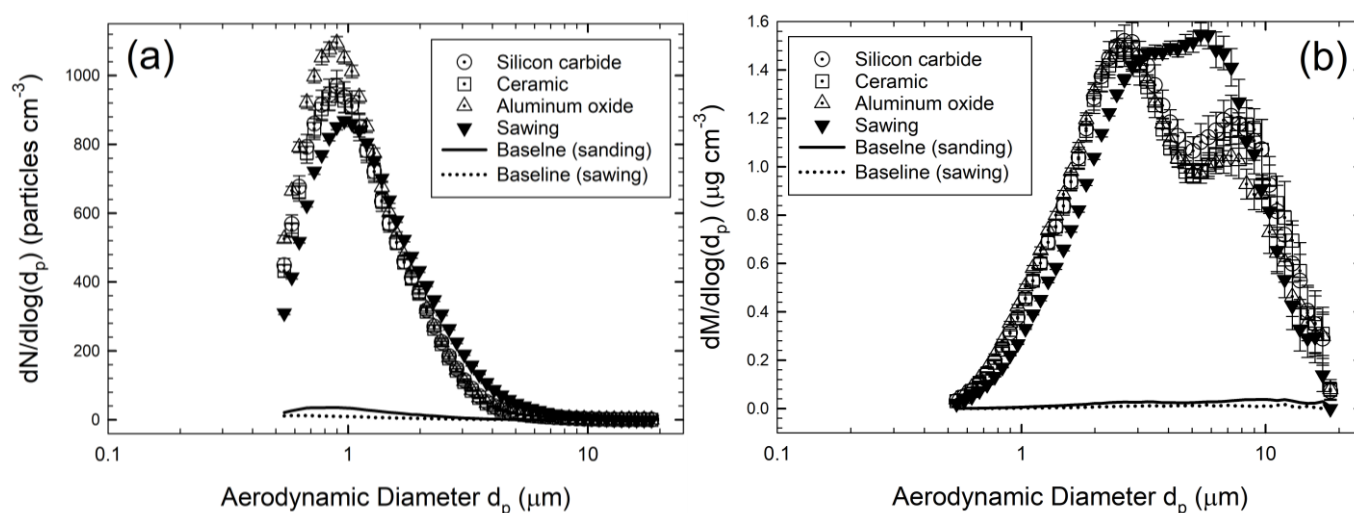

Fig. 3. (a) Number-based and (b) mass-based size distributions of the dust measured by APS from sawing and sanding (with sandpapers of ceramic, silicon carbide, and aluminum oxide) Corian®.
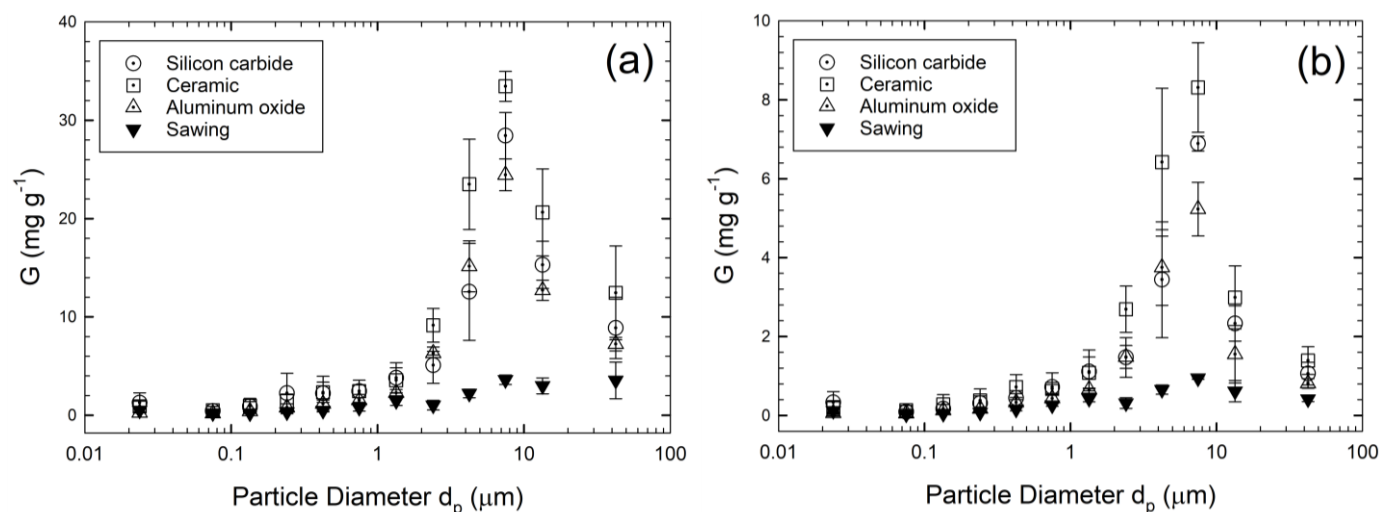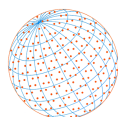
Fig. 4. The normalized generation rates of (a) airborne dust and (b) aluminum element from sawing and sanding (with sandpapers of ceramic, silicon carbide, and aluminum oxide) Corian®.

$$G_{rd} = \sum G_i \times f_i \tag{2}$$

where G_i and f_i are the dust generation rate and respirable fraction of the ith stage of MOUDI, respectively.

As shown in Table 1, the respirable dust generation rate is 5.9 from sawing and 24.9, 32.5, and 20.2 from sanding with silicone carbide, ceramic and aluminum oxide sandpapers, respectively. This indicates that sawing and sanding Corian® with silicone carbide, ceramic and aluminum oxide sandpapers results in 0.59%, 2.49%, 3.25%, and 2.02% of the removed mass becoming respirable dust, respectively.

The averaged aluminum content from the metal element analyses of three sets of MOUDI samples are presented in Fig. 5(a), showing a range between 10 and 32%. For particles smaller than 10 µm, the aluminum content does not seem to vary much with particle size. The aluminum content for particles larger than 10 µm is apparently lower than that in smaller sizes. This is possibly because larger particles may contain more acrylic polymer that is another main component of Corian®. A previous study (Qi *et al.*, 2016) also showed that the bulk dust contained lower aluminum content than the smaller airborne dust. Overall, the aluminum content for each particle size does not vary much among sawing and sanding with different sandpaper materials. By taking into account the particle size distribution in Fig. 4 and the respirable fraction, we computed the aluminum content in the respirable dust and list the results in Table 1. Clearly, the use of aluminum oxide sandpaper does not lead to a higher aluminum content in the respirable dust from sanding Corian®. Thus, we assume that all the aluminum content in the respirable dust is from the ATH in Corian®. Based on the molecular weights of aluminum and ATH, we computed the ATH content in the respirable dust and lists the results in Table 1 as well. The ATH contents in the respirable dust from sawing and sanding range from 72.8% to 84.2%, which demonstrates that ATH from Corian® is the dominant component of the respirable dust generated from both sawing and sanding this solid-surface composite.

3.2 VOC Measurement

Table 1 also lists the generation rate of MMA from sanding and sawing. It is 0.026, 0.028, and 0.022 mg g^{-1} for sanding with silicon carbide, ceramic, and aluminum oxide sandpapers, respectively, while it is significantly higher for sawing (0.069 mg g^{-1}). This difference may be caused by the temperature difference when sanding and sawing Corian®. Note that MMA has a boiling point of 101°C. The circular saw used in the sawing experiment has specified 5800 revolutions per minute (RPM), which is likely to lead to a higher temperature during operation compared to the belt sander, which runs at a much lower speed (estimated about 640 RPM). The higher temperature may lead to more VOC compounds being released during the fabrication
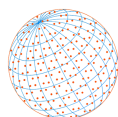
Table1. The respirable dust generation rates, aluminum and ATH contents, and respirable MMA generation rates.

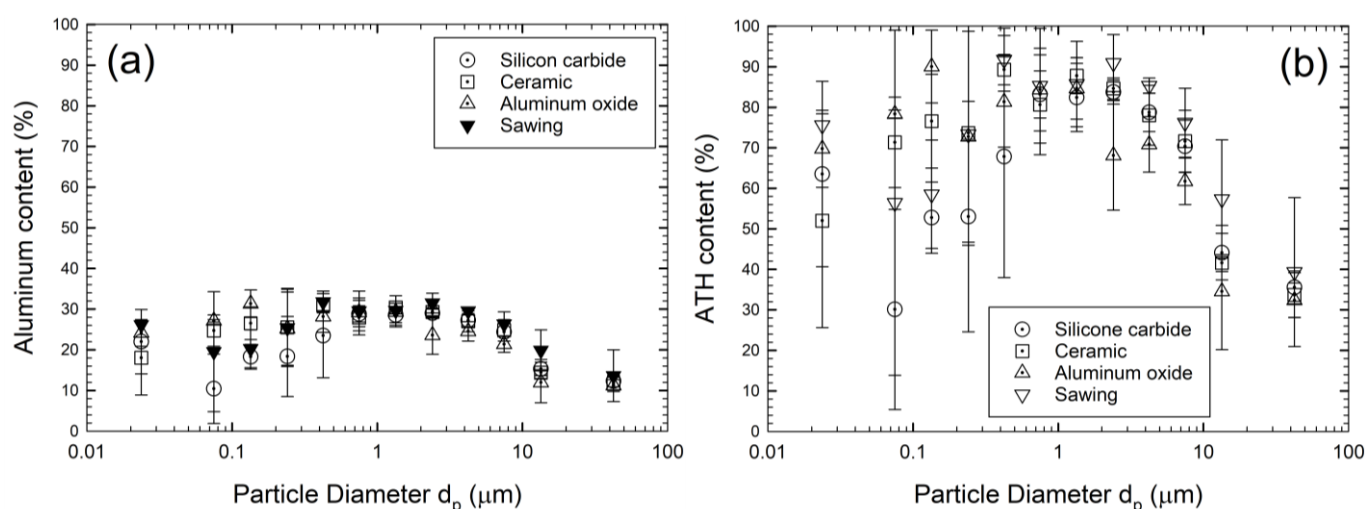|	Sanding			Sawing
	Silicon carbide	Ceramic	Aluminum Oxide	
Respirable dust generation rate (mg g^{-1})	24.9 ± 4.5	32.5 ± 7.9	20.2 ± 2.6	5.9 ± 0.7
Aluminum content (%)	25.7 ± 1.3	27.7 ± 2.2	25.2 ± 0.8	29.2 ± 1.4
ATH content (%)	74.1 ± 3.6	79.9 ± 6.4	72.8 ± 2.4	84.2 ± 4.0
Respirable MMA generation rate (mg g^{-1})	0.026 ± 0.003	0.028 ± 0.007	0.022 ± 0.007	0.069 ± 0.010

Fig. 5. (a) Aluminum element and (b) ATH contents for the dust of different sizes from sawing and sanding (with sandpapers of ceramic, silicon carbide, and aluminum oxide) Corian®.

process. The OSHA permissible exposure limit (PEL) for MMA and Particles Not Otherwise Regulated (PNOR), respirable fraction is 410 mg m^{-3} (100 parts per million) and 5 mg m^{-3}, respectively. Considering the generation rates of respirable dust and MMA during sanding and sawing Corian®, the exposure to respirable PNOR could reach its PEL much faster than the exposure to VOCs could reach their PELs, including MMA.

4 CONCLUSIONS

Laboratory tests revealed that 0.6%, 2.5%, 3.3%, and 2.0% of the mass removed from Corian® became respirable dust from sawing and sanding Corian® with sandpapers of silicon carbide, ceramic, and aluminum oxide, respectively. The particle size distribution from sawing differs from those from sanding, indicating that the size distribution of airborne dust is affected by the fabrication process. The aluminum content in the dust, however, does not vary much with the fabrication process and sandpaper materials, suggesting that the aluminum content in the dust is mainly from Corian®. The sandpaper containing aluminum oxide contributes a negligible amount of aluminum in the respirable dust when sanding Corian®. The derived ATH content of the respirable dust ranges between 72.8% and 84.2% from both sawing and sanding with all three types of sandpaper materials, verifying that ATH from Corian® is the dominant composition of the respirable dust. MMA is the main VOC from sanding Corian®, but its generation rate is much lower than that from sawing, and it does not vary much with different sandpaper materials.

FUNDING
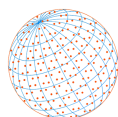
DISCLAIMER

The findings and conclusions in this report are those of the author(s) and do not necessarily represent the official position of the National Institute for Occupational Safety and Health, Centers for Disease Control and Prevention. Mention of any company or product does not constitute endorsement by the National Institute for Occupational Safety and Health, Centers for Disease Control and Prevention.

REFERENCES

Belyaev, S.P., Levin, L.M. (1974). Techniques for collection of representative aerosol samples. J. Aerosol Sci. 5, 325–338. https://doi.org/10.1016/0021-8502(74)90130-X

Brook, R.D., Rajagopalan, S., Pope III, C.A., Brook, J.R., Bhatnagar, A., Diez-Roux, A.V., Holguin, F., Hong, Y., Luepker, R.V., Mittleman, M.A., Peters, A. (2010). Particulate matter air pollution and cardiovascular disease: An update to the scientific statement from the American Heart Association. Circulation 121, 2331–2378. https://doi.org/10.1161/cir.0b013e3181dbece1

CEN (2006). Safety of machinery-evaluation of the emission of airborne hazardous substances-Part 3: Test bench method for measurement of the emission rate for a given pollutant, EN 1093-3. Brussels: Belgium: CEN.

DuPont (2018). Corian® Solid surface product overview, https://www.corian.com/IMG/pdf/k-27478_corian_solid_surface_product_overview.pdf (accessed 18 December, 2019).

Kang, S., Liang, H., Qian, Y., Qi, C. (2019). The composition of emissions from sawing Corian®, a solid surface composite material. Ann. Work Exposures Health 63, 480–483. https://doi.org/10.1093/annweh/wxz009

Kelleher, P., Pacheco, K., Newman, L.S. (2000). Inorganic dust pneumonias: The metal-related parenchymal disorders. Environ. Health Perspect. 108, 685–696. https://doi.org/10.1289/ehp.00108s4685

McKeever, R., Okaneku, J., LaSala, G.S. (2014). More on pulmonary fibrosis associated with aluminum trihydrate (Corian) dust. N. Engl. J. Med. 371, 973. https://doi.org/10.1056/nejmc1407658

NIOSH (2003a). ELEMENTS by ICP (Hot Block/HCl/HNO3 Digestion): Method 7303. NIOSH Manual of Analytical Methods (NMAM), Issue 1. National Institute for Occupational Safety and Health.

NIOSH (2003b). METHYL AND ETHYL METHACRYLATE: Method 2537. NIOSH Manual of Analytical Methods (NMAM), Issue 3. National Institute for Occupational Safety and Health.

Qi, C., Echt, A., Murata, T.K. (2016). Characterizing dust from Cutting Corian®, a solid-surface composite material, in a laboratory testing system. Ann. Occup. Hyg. 60, 638–642. https://doi.org/10.1093/annhyg/mew005

Raghu, G., Collins, B.F., Xia, D., Schmidt, R., Abraham, J.L. (2014). Pulmonary fibrosis associated with aluminum trihydrate (Corian) dust. N. Engl. J. Med. 370, 2154. https://doi.org/10.1056/nejmc1404786

Taskar, V.S., Coultas, D.B. (2006). Is idiopathic pulmonary fibrosis an environmental disease? Proc. Am. Thorac. Soc. 3: 293–298. https://doi.org/10.1513/pats.200512-131TK